IEEE Access
Multidisciplinary | Rapid Review | Open Access Journal

Received December 6, 2020, accepted January 18, 2021, date of publication February 9, 2021, date of current version February 17, 2021.

Digital Object Identifier 10.1109/ACCESS.2021.3058297

Prediction of Stroke Lesion at 90-Day Follow-Up by Fusing Raw DSC-MRI With Parametric Maps Using Deep Learning

ADRIANO PINTO[1,2], (Member, IEEE), JOANA AMORIM[1], ARSANY HAKIM[2], VICTOR ALVES[3], MAURICIO REYES[4], AND CARLOS A. SILVA[1]

[1]Center for Micro-Electro Mechanical Systems (CMEMS-UMinho), University of Minho at Azurém, 4800-058 Guimarães, Portugal
[2]Support Center for Advanced Neuroimaging, University Institute for Diagnostic and Interventional Neuroradiology, Bern University Hospital, 3010 Bern, Switzerland
[3]Centro Algoritmi, University of Minho, 4710-057 Braga, Portugal
[4]Healthcare Imaging A.I. Lab, Insel Data Science Center, Bern University Hospital, 3010 Bern, Switzerland

Corresponding author: Adriano Pinto (id6376@alunos.uminho.pt)

This work was supported by the FCT National Funds through the National Support to Research and Development Units Grant, under Project UIDB/04436/2020, Project UIDB/00319/2020, and Project UIDP/04436/2020. The work of Adriano Pinto was supported by the scholarship from the Fundação para a Ciência e Tecnologia (FCT), Portugal, under Grant PD/BD/113968/2015.

ABSTRACT Stroke is the second most common cause of death in developed countries. Rapid clinical assessment and intervention have a major impact on preventing infarct growth and consequently on patients' quality of life. Clinical interventions aim to restore perfusion deficits via pharmaceutical or mechanical intervention. Regardless of which reperfusion procedure is used, clinicians need to consider the risks and benefits based on multi-modal neuroimaging studies, such as MRI scans, as well as their own clinical experience. This intricate decision-making process would benefit from an automatic prediction of the final infarct, which would provide a estimation of tissue that will probably infarct. This paper introduces a deep learning method to automatically predict ischemic stroke tissue outcome. The authors propose an end-to-end deep learning architecture that combines information from perfusion dynamic susceptibility MRI, alongside perfusion and diffusion parametric maps. We aim to automatically extract features from the raw perfusion DSC-MRI to further complement the information gleaned from standard parametric maps, and to overcome the loss of information that can occur during perfusion postprocessing. Combining both data types in a single architecture, with dedicated paths, we achieve competitive results when predicting the final stroke infarct core lesion in the publicly available ISLES 2017 dataset.

INDEX TERMS Stroke, magnetic resonance imaging, image prediction, deep learning, DSC-MRI.

I. INTRODUCTION

Ischemic stroke is a major cause of death worldwide [1]. Acute ischemia is caused by a sudden occlusion of one (or more) of the arteries supplying blood to the brain [2], leading to a reduction of blood flow and triggering hypoperfusion with hypoxia and neuronal paralysis. This state can be reversible if timely reperfusion occurs alongside restoration of the blood flow, but if persistent occlusion occurs, it may progress to irreversible tissue damage (infarct core) [3]. Thrombolysis and mechanical thrombectomy are the established procedures for restoring tissue reperfusion to salvage tissue at risk. However, both procedures are associated with complications, including hemorrhage and vascular injury [4], [5]. Therefore, assessment of the risks and benefits for each patient and prompt identification of tissue at risk are essential factors in the success of acute stroke therapy [6]. Furthermore, several pathophysiological factors need to be considered, including location of the occlusion, other comorbidities, and the state of collateral circulation [7]. The latter is a key factor to the clinical outcome [8], [9], as vascular network with sufficient collateral flow will keep the neural cells viable until they are rescued by reperfusion therapy [8].

Correct decision-making in the management of stroke depends on the accurate differentiation of ischemic penumbra from the infarct core, requiring advanced neuroimaging,

The associate editor coordinating the review of this manuscript and approving it for publication was Michele Magno.

namely CT or MRI perfusion [10]. Both techniques detect tissue at risk. CT remains the most commonly neuroimaging technique due to its availability and rapidity. However, multi-parametric MRI is more sensitive in detecting early ischemic stroke, especially smaller ischemic lesions as well as lesions in the posterior fossa. Perfusion Dynamic Susceptibility Contrast-enhanced MRI (DSC-MRI) is used to assess the penumbra with whole brain acquisition across time, during injection of a contrast agent [10]. From stacked slices of 2D MRI acquisitions, forming a 3D volume, across a time frame, 4D spatiotemporal data is generated, where the intensity of each voxel varies across time due to the bolus passage [11]. From this data, it is possible to generate a set of standard parametric perfusion maps such as mean transit time (MTT), time-to-maximum (Tmax), time-to-peak (TTP), cerebral blood volume (CBV) and cerebral blood flow (CBF). CBF, CBV, MTT, TTP, and Tmax perfusion maps can be viewed as surrogate parametric maps that summarize the perfusion process, encompassing specific blood flow dynamics. To obtain such maps, standard approaches first require an arterial input function (AIF), that characterizes the time-concentration curve in one of the largest arteries of the brain. Then, the parametric maps are obtained by applying a deconvolution to the time-concentration curve of each voxel alongside the AIF. Since the AIF is patient-specific, the resultant parametric maps are dependent on the flow rate of injection, and more importantly dependent on the cardiovascular condition of the patient [12], [13]. However, automatically detecting a regional artery near the infarct area is not always technically feasible, due to the low resolution of the image on which the artery needs to be selected. Therefore, the location of the AIF, in clinical practice is mostly chosen in a major vessel that can be visible on the input image. This practical solution however, limits the accuracy due to known delay and dispersion effects [14]. In clinical context, where time is essential for the success of the treatment, manual detection of AIF is unfeasible [12], because stroke is a dynamic process, where in the absence of clinical intervention the hypoperfused region becomes irreversibly damaged, leading to a growth of the infarct core [10]. Predicting stroke lesion at a given time since stroke provides important information about the underlying dynamic process of a stroke lesion. In addition, it may guide physicians in their time-critical decision-making process. In this paper, we propose to automatically extract feature maps from perfusion DSC-MRI data, with the goal of complementing the standard parametric maps, and avoid the possible loss of information when generating such parametric maps. To do so, we present an end-to-end two-pathway multi-data deep learning network that considers information from the DSC-MRI perfusion acquisitions, and the standard parametric perfusion/diffusion maps to predict the stroke lesion at a 90-day follow-up.

A. PREVIOUS WORK

Several methods have already been proposed to predict the infarct core lesion based on multivariate linear regression models, decision trees, and Convolutional Neural Networks (CNNs) [15]–[18]. In addition, since Ischemic Stroke Lesion Segmentation (ISLES) 2016 & 2017 Challenges, which provide a public training dataset alongside a testing dataset evaluated by an online platform, prediction of the infarct core based on acute MRI Perfusion and Diffusion imaging has gained higher interest in the machine learning community. For a summary of the ISLES 2016 and 2017 results, please see the summary paper by [19].

The majority of the proposed methods for stroke lesion prediction only considers the standard parametric maps [19]. Only recently, perfusion DSC-MRI has been considered for final infarct stroke prediction [20]–[24]. Amorim *et al.* [20] evaluated the use of attention models when merging feature spaces extracted from standard parametric perfusion and diffusion maps, and perfusion DSC-MRI acquisitions. Based on the DSC-MRI simulator proposed by [25], Debs *et al.* [23] employs the simulator as a synthetic data generator to increase the robustness of a simple fully-connected CNN architecture. The encoding of the perfusion images is achieved by extracting 2D patches, where the first dimension comprehends the unrolled Moore's neighbourhood and the second one the temporal DSC-MRI acquisitions. By adding clinically relevant data, the authors argue the need for fewer real training data to robustly predict the final infarct lesion. Using a similar data encoding, Giacalone *et al.* [22] extracts temporal texture features from the local binary pattern, which are then fed to a support vector machine to classify the chances of survivability of each voxel. Both proposals perform prediction of the final infarct lesion at 30-days, on a small testing patient cohort, where the acquisition protocol needs to be restrained to 60 temporal acquisitions. Moreover, the majority of the testing set encompasses patients who didn't receive thrombolytic therapy, therefore, the testing data covers only the patients in whom the probability of irreversible tissue damage is higher. Ho *et al.* [26], similarly to our work, proposed a deep learning architecture that simultaneously captures spatio-temporal information, designated CNN-contralateral. From pairs of patches that contain the patch of interest and its contralateral patch, the authors first focus on extracting temporal information. Hence, a 2D convolutional layer is applied to each element of the input pair, being the third dimension of the 3D filter equal to the number of temporal acquisitions. Afterwards, both outputs are summed encoding the temporal information as channels and the data is processed along the spatial dimensions. The results obtained in a private dataset of 48 patients demonstrate the importance of the proposal. However, the prediction of the stroke lesion is performed in a short time-window of 3-7 days after treatment. Instead of using DSC-MRI, but still performing prediction of the final stroke lesion, Robben *et al.* [27] considered spatio-temporal CT perfusion. The authors demonstrated the capacity to avoid standard deconvolution processing methods by using the spatio-temporal data directly as input to a Deep Learning neural architecture based on the one

proposed by Kamnitsas *et al*. [28]. In addition, the method of Robben *et al*. [27] combines imaging with clinical metadata, increasing its performance. Although not applied to stroke lesion prediction, there are approaches that aim to achieve a higher level of abstraction from the perfusion DSC-MRI [29], [30]. Hess *et al*. [30] developed a deep learning architecture to avoid the need for a deconvolution step. The method aims to generate improved versions of standard parametric maps from an automatic machine learning approach, which are independent of the underlying mathematical foundations and drawbacks of the deconvolution.

B. CONTRIBUTIONS

This paper extends our previous work [21], presented at the MICCAI conference, where the basic concept and methodology was presented along with preliminary results. In this paper, we present an improved automatic multi-data deep learning network for predicting the final infarct lesion, from DSC-MRI perfusion and standard parametric maps. Since standard perfusion and diffusion maps are generated from kinetic models, we hypothesize that complementary information to the standard clinical maps can be extracted from the raw perfusion data to improve stroke outcome prediction. Compared to our preliminary results presented in Pinto *et al*. [21], where various training stages per block were required, here we propose an end-to-end training that combines the information from the standard parametric maps and the DSC-MRI simultaneously, which enables a better interplay between features from different sources, improving lesion outcome prediction.

Another contribution of our work is a fully automatic pipeline that does not require the determination of a patient-specific AIF when dealing with DSC-MRI data. In our proposal, the temporal information is encoded as channels, where a deep neural network is responsible for extracting spatio-temporal information of relevance, avoiding the spatial variability associated with the definition of a reference input function.

The remainder of the paper is organized in five sections. Section II describes the methodology. Section III addresses the setup for final infarct core tissue prediction. Section IV addresses the discussion of the results. Finally, Section V presents the main conclusions.

II. METHODOLOGY

In this section, we first describe the perfusion dynamics associated with the DSC-MRI for ischemic stroke. Afterwards, we detail the proposed two pathway deep learning architecture, which aims to combine the features extracted from the DSC-MRI acquisitions with the features extracted from the standard parametric perfusion and diffusion maps. Our motivation is to obtain a model aware of underlying phenomena in ischemic stroke lesion across time, therefore capable of predicting the final infarct lesion from perfusion DSC-MRI, clinical maps.

A. PERFUSION DSC-MRI IN ISCHEMIC STROKE

In the acquisition of the perfusion DSC-MRI, the arrival of contrasting agent to the brain, the bolus, is responsible for a drop on the MRI signal, and consequently for attenuating the intensity values. The intensity attenuation is recovered as the contrast agent is diluted by the circulation. This behavior can be described by a time-attenuation curve. In the presence of an ischemic stroke, the bolus passage in the infarct core region is mostly absent, so its intensity values barely change across time. However, we may observe an attenuation of the intensities in the hypo-perfused tissue due to residual blood flow circulation or bolus dispersion [8], [31]. Figure 1a depicts the signal intensity behavior in a patient with an acute ischemic stroke, during contrast agent injection. In each voxel, the time-attenuation curve corresponds to a time-concentration curve, since a higher intensity attenuation corresponds to higher concentration of contrasting agent.

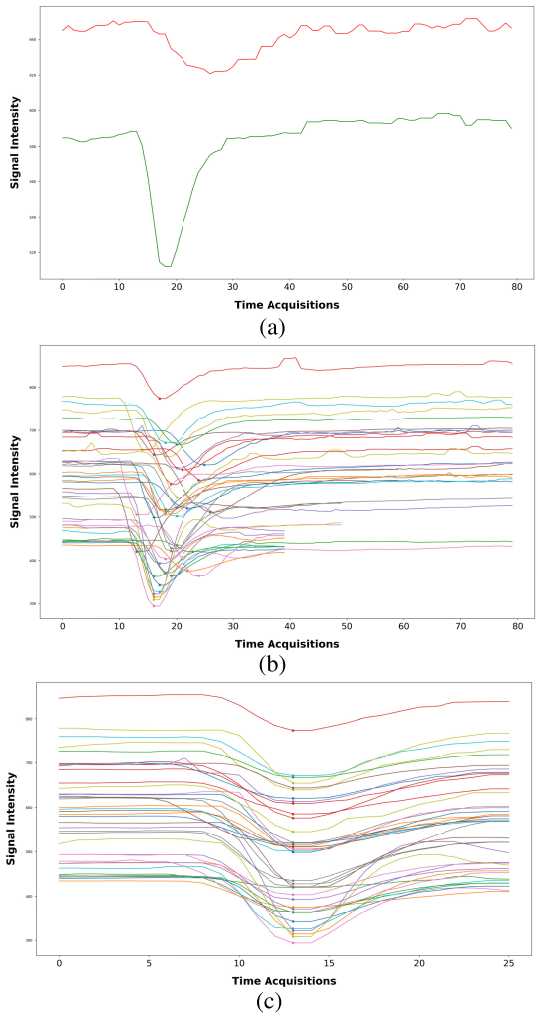

FIGURE 1. Perfusion DSC-MRI time-attenuation curve of: (1a) an acute ischemic stroke patient in the healthy tissue (green) and in the final infarct core (red); (1b) DSC-MRI signal of acute ischemic patients before applying the temporal pre-processing, and (1c) after extracting an aligned subset of temporal acquisitions.

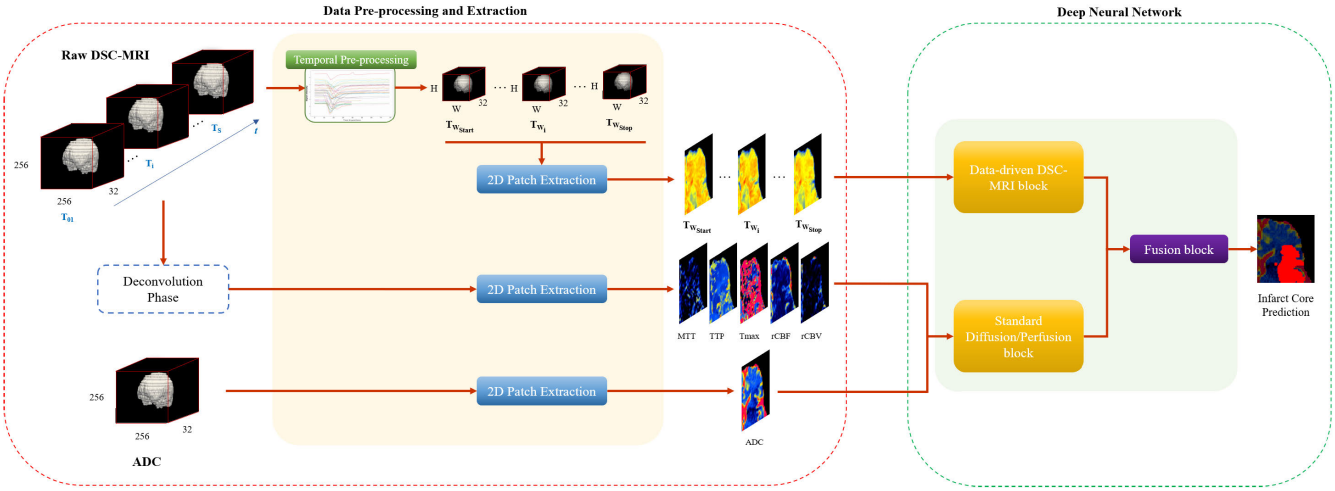

FIGURE 2. **Proposed pipeline that considers the raw-DSC-MRI data, along with standard parametric maps of perfusion and diffusion in a two-pathway deep neural network. Intersection of paths comprehends concatenation of data.**

Based on this observation it is possible through deconvolution in time-space to obtain 3D MRI perfusion maps that characterize different cerebral perfusion properties.

However, as can be seen in Figure 1b, there is a misalignment in the temporal steps of the DSC-MRI. This misalignment will affect the training of deep neural networks. To surpass this dispersion, we propose to align the DSC-MRI scans across all patients by identifying and selecting a common temporal window where the bolus passage occurred, as shown in Figure 1c. We focus on identifying the time-stamp where the average of intensities in the whole brain is the lowest, corresponding to the highest signal attenuation and therefore the highest concentration of contrast agent in the brain. This time-stamp characterizes the point in time when the differences of perfusion between healthy tissue, ill-perfused tissue and infarct core tissues are higher [12]. We use the information on the time-step with the highest concentration to define a temporal window of size $\mathcal{W}$ centred on it. The method is encompassed by the temporal pre-processing block shown in Figure 2, in the data-processing and extraction module. After, the 3D MRI acquisitions contained in the selected time window undergo a bi-dimensional patch extraction, which is used as the input of the neural network module (Figure 2), particularly the data-driven DSC-MRI block where the temporal dimension is modelled as channels.

B. DEEP LEARNING ARCHITECTURE

Based on neuroimaging scans acquired at the acute phase, we assign to each MRI voxel one of two classes: healthy tissue or stroke tissue that will appear as infarct at the 90-day follow-up. To predict the final infarct core volume, the deep learning module, shown in Figure 2, encompasses three functional blocks: data-driven block, standard diffusion/perfusion block and fusion block. The data-driven and standard diffusion/perfusion blocks generate features from two diverse groups of MRI data in parallel paths of the network. On one hand, the standard diffusion/perfusion block extracts features directly from 2D MRI patches of parametric maps, where the perfusion maps result from a deconvolution step applied to the raw DSC-MRI data. The deconvolution was performed offline at the onset time acquisition, by a third party software. On the other hand, the data-driven branch computes features from DSC-MRI data. Given the different extracted feature sets, the fusion block aggregates and elaborates over the two inputs, as shown in Figure 2.

1) DATA-DRIVEN DSC-MRI BLOCK

The spatio-temporal information provided by the perfusion DSC-MRI is considered in the Data-driven block. After temporal standardization, 2D patches are extracted for the selected time-acquisitions serving as input to the architecture. We propose to characterize the tissue at risk of infarction by capturing information of the blood dynamics using the temporal information of DSC-MRI sequences. This is performed by encoding the temporal sequence as input channels of the neural network. The temporal correlation is further enforced at the scaling up of the decoder path where the network performs up-sampling followed by a convolution layer, with a kernel of $(1 \times 1 \times C_s)$ where C_s denotes the number of channels at the upper scale s. Thus, features extracted along the temporal and local dimensions, by convolutional layers with kernels of (3×3), are further correlated and combined along different scales of the decoder path, aiming to extract discriminative blood flow information.

2) STANDARD DIFFUSION/PERFUSION BLOCK

The standard diffusion/perfusion block encompasses the standard parametric maps of perfusion: Tmax, TTP, MTT, relative-CBV (rCBV), and relative- (rCBF), computed based on the perfusion DSC-MRI with standard deconvolution methods [11], [12], and the Apparent Diffusion

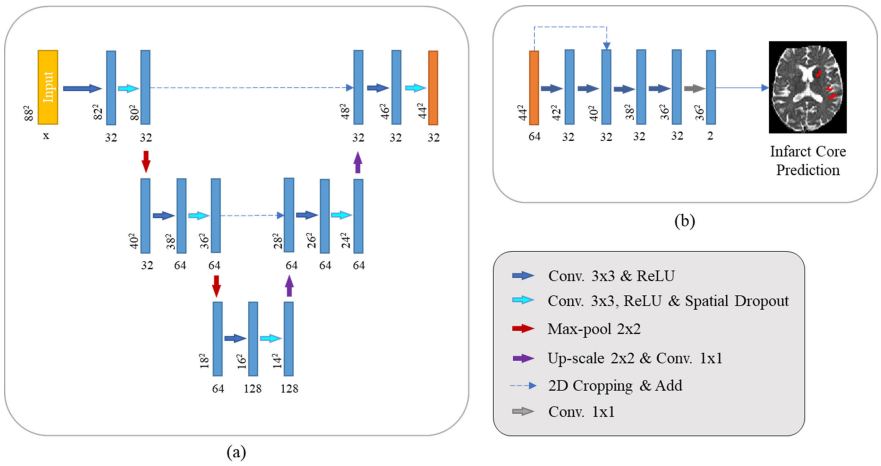

FIGURE 3. Deep neural network architectures applied to: (a) - the standard diffusion/perfusion block and the data-driven DSC-MRI block, and (b) to the fusion block. Figure 3a shows a U-Net based architecture, while Figure 3b details the FCNN network.

Coefficient (ADC) map. This block is functionally equivalent to other state-of-the-art approaches, mimicking the architecture proposed for the Data-driven DSC-MRI block. The input of the block are 2D patches extracted across the parametric maps.

3) FUSION BLOCK

To take advantage of the distinct information captured in the Data-driven DSC-MRI and in the Standard diffusion/perfusion block, we combine the feature maps from the last scale of each decoder and combine them into a short FCNN path. Merging information from both types of data allows the network to consider complementary information that might improve the prediction of the final stroke lesion. The fusion block considers four convolutional layers with a residual connection at the second layer. The outputs of the fourth layer are fed to the softmax classifier.

The data-driven and the standard diffusion/perfusion blocks are based on the 2D U-Net architecture [32], which has proved to be competitive in many biomedical image applications. All scales of the architecture consider small convolutional kernels of size 3×3. The convolutional layers of the first scale have 32 channels, whereas at the second and third scales the number of channels is 64 and 128, respectively. Each convolutional layer comprises a convolutional operation, combined with ReLU activation function [33]. Spatial dropout is applied at every two convolutional layers, with a probability of $p = 0.25$ [34]. Long skip connections are employed at the first and second scales, between the encoder and decoder paths. Figure 3 shows the proposed architecture.

III. EXPERIMENTAL SETUP

Our method was evaluated on the publicly available ISLES dataset [35], which is associated with an online benchmark platform responsible for the evaluation of the testing set data. In this section, we detail the dataset used and the metrics employed for evaluation. Lastly, we describe the model training and parameters of the network.

A. DATA

ISLES 2017 dataset encompasses 75 ischemic stroke patients, which are separated into two sets: training ($n = 43$) and testing ($n = 32$). Both sets are constituted by patients who underwent mechanical thrombectomy, and are characterized by perfusion DSC-MRI and its standard 3D perfusion parametric maps, which are the relative CBV (rCBV), relative CBF (rCBF), MTT, TTP, and Tmax, alongside a 3D diffusion map, the ADC. Alongside the MRI acquisitions, the dataset contains the manual delineation of the final infarct lesion from a 90-day follow-up T2-weighted MRI. However, only for the training set the ground truth is disclosed for public access. Hence, the evaluation of the testing set can only be performed by the online platform [35].

When assessing the DSC-MRI data, we noticed that the training set has four cases where the acquisition might have been corrupted (cases 31, 42, 43, 45). Consequently, the proposed temporal slicing and alignment method is not able to select an appropriate time-window, despite these cases possess viable standard parametric maps. So, we have excluded these cases from the training set. In all the experiments, a total of 39 cases were used as training set. Using cross-validation, the window size was selected as $\mathcal{W} = 26$.

B. EVALUATION

For evaluation purposes we used the same metrics defined for ISLES Challenges [19]: Dice score, Hausdorff Distance (HD), Average Symmetric Surface Distance (ASSD), Precision, and Recall.

HD allows the identification of the farthest spatial outlier present in the prediction. The remaining distance metric, ASSD, computes the average distances between volumes' surface points, namely the ground truth and the prediction.

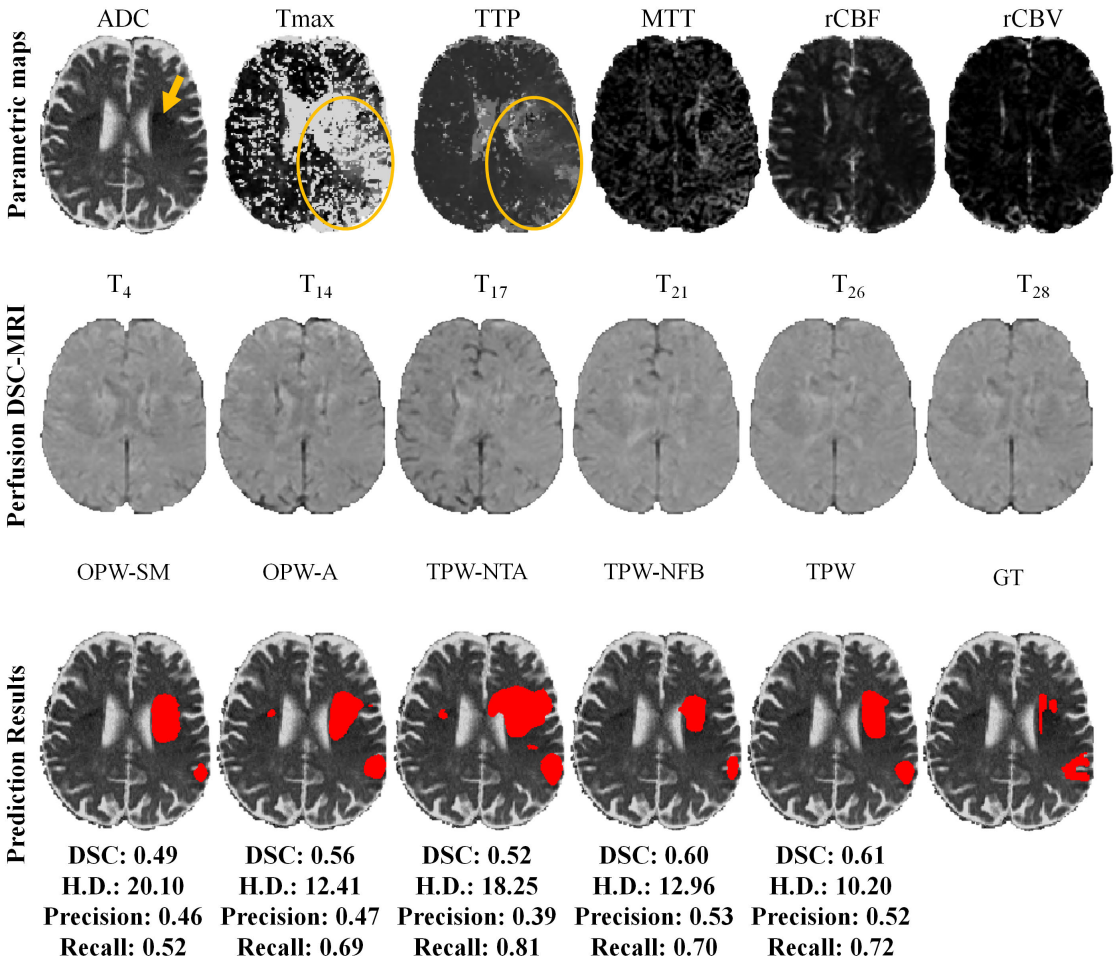

FIGURE 4. MRI of a 75-year-old male patient performed 83 minutes after acute onset of right hemiplegia, NIHSS 22. The MRI depicted occlusion of the M1 segment of the left middle cerebral artery (not shown), as well as diffusion restriction in the middle cerebral artery territory and the basal ganglia as shown in the ADC map (arrow). DSC perfusion showing prolongation of the temporal parameters, as seen in Tmax, TTP and MTT. The ground truth is the delineation of the final infarct as seen on the follow-up imaging three months after the initial stroke. In the bottom row, from left to right we show the results obtained from the one-pathway with standard parametric maps (OPW-SM), the one-pathway with all imaging data (OPW-A), two-pathway with no temporal slicing (TPW-NTA), the two-pathway without fusion block (TPW-NFB), our proposal (TPW), and the ground-truth at a 90-day follow-up.

Dice score measures the spatial overlap between two volumes. Precision characterizes the probability of assigning correctly a given class, while Recall consists of a probability in identifying positive cases as such.

C. PRE- AND POST-PROCESSING

All MRI data is already co-registered and skull-stripped [19]. Figure 4 shows a training case example with the standard parametric maps alongside some temporal acquisitions of perfusion DSC-MRI and the manual segmentation of the tissue lesion, the Ground Truth (GT).

As preprocessing, we first resize all MRI data to the same volume space of $256 \times 256 \times 32$, since the dataset contains acquisitions from different centers. Bias field correction was performed to the perfusion DSC-MRI using the N4ITK method [36], followed by a temporal processing that extracts a fixed temporal window size of 26 acquisitions, which is based on the sampling rate of the MRI acquisition. Finally, a linear scaling was applied between $[0, 255]$ to all maps. Before linear scaling, the T_{max} was clipped to $[0, 20s]$, and the ADC was clipped to the range $[0, 2600] \times 10^{-6} mm^2/s$, as values out of these ranges are known to be biologically meaningless [17].

D. MODEL TRAINING AND PARAMETERS

The overall architecture, including both blocks, was trained with 35 cases, alongside a validation set encompassed by 4 cases, randomly chosen. In each case, 1000 patches of dimensions 84×84 were randomly extracted. The network was trained with ADAM optimizer ($\text{lr} = 1 \times 10^{-5}$) and a mini-batch of size 4. For regularization, we employed a spatial drop-out [34] of 0.25 at each two convolutions. We used

TABLE 1. Results in ISLES 2017 testing dataset for the different configurations of our proposal. Each metric contains the mean ± standard deviation. Underlined values correspond to the highest score of the respective performance metric (column-wise).

Experiments	Params.	Dice	H.D.	ASSD	Precision	Recall
OPW-SM – One-pathway standard maps (Baseline)	382 154	0.30 ± 0.21	38.83 ± 21.10	7.08 ± 5.15	0.26 ± 0.23	0.64 ± 0.30
OPW-A – One-pathway	816 916	0.28 ± 0.21	37.47 ± 16.05	6.90 ± 4.43	0.32 ± 0.28	0.54 ± 0.30
TPW-NTA – Two-pathway no temporal align	838 594	0.28 ± 0.21	43.66 ± 23.57	7.89 ± 6.31	0.25 ± 0.23	0.66 ± 0.33
TPW-NFB – Two-pathway no fusion block	787 778	0.27 ± 0.21	40.89 ± 18.68	8.21 ± 6.68	0.28 ± 0.26	0.53 ± 0.34
TPW-PM – Two-pathway with parametric maps	828 514	0.28 ± 0.23	44.13 ± 19.98	8.39 ± 7.30	0.26 ± 0.26	0.64 ± 0.31
TPW-AD – Two-pathway with DSC-MRI and ADC	834 562	0.26 ± 0.22	44.29 ± 17.97	7.28 ± 4.30	0.27 ± 0.27	0.66 ± 0.30
3PW – Three-pathway	1 177 058	0.28 ± 0.21	40.12 ± 14.50	6.74 ± 3.85	0.28 ± 0.25	0.59 ± 0.29
TPW – Two-pathway **(Proposal)**	836 002	0.31 ± 0.21	33.94 ± 17.43	5.99 ± 4.58	0.29 ± 0.23	0.63 ± 0.30

the soft-dice loss function [37], where the gradient of the Dice score for the j^{th} voxel of prediction is given by:

$$\frac{\delta Dice}{\delta p_j} = \frac{g_j(\sum_i^N p_i^2 + \sum_i^N g_i^2) - 2p_j \sum_i^N p_i g_i}{(\sum_i^N p_i^2 + \sum_i^N g_i^2)^2} \quad (1)$$

The sum is performed for the N voxels of the output patch, where $p_i \in P$ denotes the predicted probability of a voxel i and $g_i \in G$ the respective ground-truth label.

All the models were developed using Keras with Tensorflow, and trained on an Nvidia GeForce GTX 1070 8 GB, with a prediction time around 15 seconds.[1]

IV. RESULTS AND DISCUSSION

This section starts by discussing the ablative study, which measures the importance of the main contributions of our proposal. In this ablative study, we first evaluate the importance of including spatio-temporal imaging data with the standard parametric maps. Second, we measure the importance of the two-pathway architecture and key components of the method, namely the temporal processing of the perfusion DSC-MRI and the data-fusion block. After, we delve in the information extracted from the DSC-MRI deep neural network. Finally, we compare our proposal with state-of-the-art methods in ISLES 2017 Challenge.

A. ABLATION STUDY

To measure the importance of the key components of our proposal, we start by evaluating the impact of considering the DSC-MRI data alongside the standard parametric maps. Then, we compare our two-pathway architecture with the one-pathway based on the U-Net. Finally, we measure the impact of performing the temporal processing of the DSC-MRI and of the Fusion block. The results are presented in Table 1.

1) ON THE INCLUSION OF SPATIO-TEMPORAL IMAGING DATA

We evaluate the importance of using one-pathway with the standard maps (OPW-SM) compared to a two-pathway architecture (TPW) that combines the DSC-MRI with the standard maps. The results are presented in Table 1. Comparing the two experiments, we verified the benefit of combining both types of input. The TPW achieved higher average Dice score, alongside lower average distance metrics and higher average Precision score. We know that the parametric maps are obtained by summarizing the dynamics of the time-attenuation curve through different processes [38]. So, while the standard diffusion/perfusion block extracts information on this rich set of inputs, the data-driven DSC-MRI block takes an unbiased look at the raw data by considering only the time-attenuation curve conditioned on the information of the viability of the brain tissue — healthy or lesioned tissue after 90-day. This may have allowed the block to learn a new set of features, boosting the performance of the model. Thus, we may conclude that direct extraction of features from the DSC-MRI data was important to predict the final infarct stroke lesion.

2) ONE PATHWAY *OR* TWO-PATHWAY

In this ablative study, we evaluate how the DSC-MRI and the standard parametric maps can be aggregated in our neural network. This combination can be performed in two different ways. We can directly aggregate both input data into a single network (OPW-A), allowing the network to relate information from different types of data; or, we can use different paths (TPW) to extract specific features that are combined later. The results of this study are presented in Table 1. In this study both methods employed the same temporal slicing and alignment. From the results, it is possible to verify that using a single path (OPW-A) achieved lower performance in all metrics except in the average Precision. Considering our data, we observe that while the parametric MRI maps summary different aspects of the dynamics of the time-attenuation curve, in DSC-MRI each input characterizes a specific time step. So, we hypothesize that since in TPW there is a specific path for each type of input, the use of a dedicated path allowed generating better features. So, in the context of predicting stroke lesion evolution, we conclude that the use of dedicated paths to extract information from distinct physiological processes is more effective than using a single network to process all of them simultaneously.

[1]The source code for reproducing the segmentations, the models' weights can be found at: https://github.com/apinto92/DSCMRI_Stroke_Prediction.git.

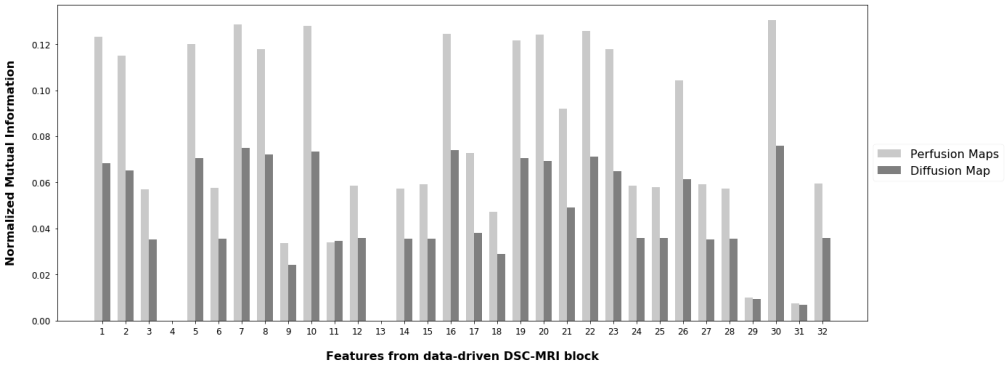

FIGURE 5. Normalized Mutual Information between the standard perfusion/diffusion maps and the feature maps from the data-driven block for the training set.

3) THE IMPORTANCE OF TEMPORAL ALIGNMENT AND THE FUSION BLOCK

In this study, we evaluate the importance of two components of our proposal, the temporal slicing and alignment, and the fusion block. In the comparison of the temporal slicing and alignment, the data-driven branch uses the first 40 temporal acquisitions. This was the minimum number of slices available across all patients in the dataset. The results are presented in Table 1. We verify that elaborating with more convolutional layers over the features aggregated from both paths (TPW), instead of removing the fusion block (TPW-NFB), provides an overall increase of the performance. Comparing the metrics, we note an increase in the average Dice, average Precision and Recall. Regarding the temporal alignment, we observe that TPW outperforms TPW-NTA, presenting an increase in the average Dice score, alongside lower average distance metrics. Hence, we conclude that performing temporal slicing and alignment allows a spatio-temporal standardization useful for the extraction of higher discriminative features when predicting the final infarct stroke lesion. Furthermore, the spatio-temporal standardization provides a reduction on the amount of temporal acquisitions used as input, without impairing the performance of the method.

4) INDEPENDENT BRANCHES ACCORDING TO MRI DATA TYPE

Diffusion imaging characterizes the onset infarct tissue, providing information of lesioned brain tissue that will be encompassed by the final stroke lesion. Perfusion imaging provides richer information of salvageable surrounding tissue that is of utmost importance when predicting the evolution of this lesion [39]. However, we hypothesize that how one combines these imaging data may have impact on the quality of the prediction. Hence, in this last study, we evaluate the impact of combining either DSC-MRI and/or parametric perfusion data with diffusion data in different paths as opposed to our proposal. This study starts by having as architecture our proposed two-pathway network, while the input data varies. In one hand, we consider the DSC-MRI with the ADC (TPW-AD), while in the other, the input encompasses the perfusion maps with the ADC (TPW-PM). With the TPW-PM, the results demonstrate that considering the ADC map and the perfusion parametric maps in distinct paths, leads to an overall lower performance. This can be explained by the filters learned in the two-paths, which do not consider simultaneously perfusion/diffusion information. The TPW-AD method achieved an even overall lower performance. Combining both results, this study indicates that the ADC map, when used in a dedicated path, might require fewer data processing and/or a path specific loss function. However, when the diffusion and perfusion maps are combined at the input of the network (TPW), the overall performance improves. Finally, we also study the impact of having the same input data as in our proposed architecture but using the ADC in an independent path (3PW) that overall resulted in a lower performance.

B. DATA DRIVEN BRANCH – FEATURE ANALYSIS

In our proposal, we hypothesize that the inclusion of the source DSC-MRI data, responsible for generating the standard perfusion maps, provides additional and complementary perfusion dynamics information useful for predicting the final infarct core lesion. Henceforth, to assess the relevance of the feature space extracted from the data-driven block, we study the correlation among the features extracted from the source DSC-MRI branch and the standard perfusion and diffusion maps. The correlation is studied using the normalized mutual information, Figure 5.

As illustrated in Figure 5, the normalized mutual information achieved low association values (less than 0.2) among the extracted feature maps and the standard parametric maps. Note that values closer to 0 mean low mutual information and closer to 1 represent a high association. Regardless of the fact that the DSC-MRI acquisition only characterizes perfusion properties, we extended our analysis to both major vascular properties, diffusion and perfusion. Therefore, in the light of the performance results obtained in the testing set, we hypothesize that both functional blocks introduce distinct and complementary features, useful when predicting the final infarct core volume.

TABLE 2. Recently published methods in ISLES 2017 testing dataset and our proposal, in descending order of Dice score. Each metric contains the mean ± standard deviation. Underlined values correspond to the highest score of the respective performance metric (column-wise).

		Dice	H. D.	ASSD	Precision	Recall
Ensemble	Mok *et al.* *	<u>0.32</u> ± 0.23	40.74 ± 27.23	8.97 ± 9.52	0.34 ± 0.27	0.39 ± 0.27
	Kwon *et al.* *	0.31 ± 0.23	45.26 ± 21.04	7.91 ± 7.31	0.36 ± 0.27	0.45 ± 0.30
	Robben *et al.* *	0.27 ± 0.22	37.84 ± 17.75	6.72 ± 4.10	<u>0.44</u> ± 0.32	0.39 ± 0.31
	Pisov *et al.* *	0.27 ± 0.20	49.24 ± 32.15	9.49 ± 10.56	0.31 ± 0.27	0.39 ± 029
Single Model	Monteiro *et al.* *	0.30 ± 0.22	46.60 ± 17.50	6.31 ± 4.05	0.34 ± 0.27	0.51 ± 0.30
	Pinto *et al.* [21]	0.29 ± 0.21	41.58 ± 22.04	7.69 ± 5.71	0.21 ± 0.21	<u>0.66</u> ± 0.29
	Amorim *et al.* [20]	0.29 ± 0.21	38.90 ± 20.00	7.00 ± 4.31	0.26 ± 0.23	0.61 ± 0.28
	Lucas *et al.* *	0.29 ± 0.21	<u>33.85</u> ± 16.82	6.81 ± 7.18	0.34 ± 0.26	0.51 ± 0.32
	Choi *et al.* *	0.28 ± 0.22	43.89 ± 20.70	8.88 ± 8.19	0.36 ± 0.31	0.41 ± 0.31
	Niu *et al.* *	0.26 ± 0.20	48.88 ± 11.20	6.26 ± 3.02	0.28 ± 0.25	0.56 ± 0.26
	Sedlar *et al.* *	0.20 ± 0.19	58.30 ± 20.02	11.19 ± 9.10	0.23 ± 0.24	0.40 ± 0.29
	Rivera *et al.* *	0.19 ± 0.16	63.58 ± 18.58	11.13 ± 7.89	0.27 ± 0.25	0.21 ± 0.17
	Islam *et al.* *	0.19 ± 0.18	64.15 ± 28.51	14.17 ± 15.80	0.29 ± 0.28	0.25 ± 0.25
	Chengwei *et al.* *	0.18 ± 0.17	65.95 ± 25.94	9.22 ± 6.99	0.37 ± 0.30	0.21 ± 0.23
	Yoon *et al.* *	0.17 ± 0.16	45.23 ± 19.14	12.43 ± 11.01	0.23 ± 0.27	0.36 ± 0.32
	Baseline	0.30 ± 0.21	38.83 ± 21.10	7.08 ± 5.15	0.26 ± 0.23	0.64 ± 0.30
	Proposed	0.31 ± 0.21	33.94 ± 17.43	<u>5.99</u> ± 4.58	0.29 ± 0.23	0.63 ± 0.30

* Results retrieved from [19].

Figure 4 depicts an example case of the validation set when considering the one-pathway multi-data network, the two-pathway multi-data with no temporal slicing, and our proposal. Analyzing Fig. 4, the OPW experiment achieved the lowest Dice score and highest Hausdorff distance, when compared with the other methods. The TPW-NTA predic ted the largest final stroke lesion among the evaluated methods, which explains the high Recall metric. The TPW method yields the best prediction of the final stroke lesion, achieving the highest Dice score alongside a good balance between Precision and Recall. Additionally, the Hausdorff distance achieved by our proposal was the lowest.

C. ISLES 2017 CHALLENGE

On Table 2, we compare our proposal with state-of-the-art methods submitted to the online ISLES 2017 benchmark. It was not possible to compute statistical significance tests, since individual testing metrics are not available. Regardless of the model topology, predicting final infarct core is still a challenging and intricate task, that needs to consider scenarios of successful and unsuccessful reperfusion. Furthermore, in each reperfusion scenario, predicting the infarct growth, and consequently the final stroke lesion, needs to consider various haemodynamic factors (*e.g.* location or collateral circulation) which hinders the learning process. We emphasize that ISLES 2018 aims to segment the stroke lesion using CTP imaging, while ISLES 2017 aims to predict the stroke lesion 90-days after the onset MRI scan.

In ISLES 2017 testing set, our proposed approach was capable of achieving competitive results, with a Dice score among the top 2 ranked methods, tied with Kwon *et al.*, and with the second lowest average Hausdorff distance and the lowest average ASSD. However, we note that Kwon *et al.* used an ensemble of 12 neural networks combining Fully Convolutional Neural Networks (FCNNs) and Fully-Connected Networks (FCNs), while our proposal is a single FCNN with two branches in the input.

When comparing with ensemble strategies, we achieved lower average Dice score, when compared against Mok *et al.*, surpassing the remaining ensemble strategies. Furthermore, for a single model approach, we remark the consistency of the proposed approach, as shown by the distance metrics, being lower than all ensemble methods. As for the precision and recall metrics, we observe a slight trade-off. Considering the top two ensemble approaches, our model achieved higher average recall, alongside the lowest average precision. Comparing with Robben *et al.* and Pisov *et al.*, ensemble approaches of convolutional neural networks, our method was capable of surpassing both in the average Dice score. Similarly, we also achieved higher recall, combined with lower Hausdorff distance, on average.

Considering only single system strategies (non-ensembles), we observe that our proposal achieved the highest Dice average in the testing set. In this group, the precision and recall metrics ranked 5th and 2nd, respectively. In addition, we remark the robustness of our proposal in predicting stroke tissue outcome, observed by the low standard deviation values. We emphasize the benefits of the proposed approach to extract and model information that might not be fully characterized by the standard perfusion and diffusion maps alone.

V. CONCLUSION

In the presence of an ischemic stroke perfusion DSC-MRI data provides spatio-temporal information useful to characterize brain tissue viability and its hemodynamics. However,

due to the high amount of generated imaging data, postprocessing methods were developed to summarize the DSC-MRI in 3D parametric maps that in turn can be rapidly inspected by clinicians at onset time. Nonetheless, current postprocessing methods can provide non-physiological results and can lead to the loss of valuable information. So, in this work, we proposed a two-pathway deep neural network to simultaneously extract features from the DSC-MRI and the standard parametric maps of diffusion/perfusion. Our ablative studies demonstrate the importance of combining both types of data in dedicated paths, rather than in a single-pathway architecture. Furthermore, instead of applying the DSC-MRI data to the network, we showed that our proposed temporal slicing and alignment provides a common temporal scale beneficial to the extraction of richer features.

When evaluated on ISLES 2017 testing set, our proposal demonstrated an overall improvement when considering both types of data. From a single FCNN model we were able to achieve competitive results reaching the second highest average Dice score and lower distance metrics, surpassing some ensemble methods.

With this work, we aim to contribute in developing new methods to support clinicians during their decision process, which ponders whether to perform or not therapeutic intervention. Nonetheless, there are still open lines of research. We envision that the processing of DSC-MRI spatio-temporal data can be further consolidated so it can consider patient specific hemodynamic and also be less dependent on the acquisition protocol.

REFERENCES

[1] *Global Status Report on Noncommunicable Diseases 2014*, World Health Organization, Geneva, Switzerland, 2014.

[2] R. A. Grysiewicz, K. Thomas, and D. K. Pandey, "Epidemiology of ischemic and hemorrhagic stroke: Incidence, prevalence, mortality, and risk factors," *Neurologic Clinics*, vol. 26, no. 4, pp. 871–895, Nov. 2008.

[3] H. Memezawa, M. L. Smith, and B. K. Siesjö, "Penumbral tissues salvaged by reperfusion following middle cerebral artery occlusion in rats," *Stroke*, vol. 23, no. 4, pp. 552–559, Apr. 1992.

[4] J. S. Balami, P. M. White, P. J. Mcmeekin, G. A. Ford, and A. M. Buchan, "Complications of endovascular treatment for acute ischemic stroke: Prevention and management," *Int. J. Stroke*, vol. 13, no. 4, pp. 348–361, Jun. 2018.

[5] D. J. Miller, J. R. Simpson, and B. Silver, "Safety of thrombolysis in acute ischemic stroke: A review of complications, risk factors, and newer technologies," *Neurohospitalist*, vol. 1, no. 3, pp. 138–147, Jul. 2011.

[6] W. J. Powers, A. A. Rabinstein, T. Ackerson, O. M. Adevoe, N. C. Bambakidis, and K. Becker, "2018 guidelines for the early management of patients with acute ischemic stroke: A guideline for healthcare professionals from the American heart association/American stroke association," *J. Vascular Surg.*, vol. 67, no. 6, p. 1934, Jun. 2018.

[7] D. S. Liebeskind, R. Jahan, R. G. Nogueira, O. O. Zaidat, and J. L. Saver, "Impact of collaterals on successful revascularization in solitaire FR with the intention for thrombectomy," *Stroke*, vol. 45, no. 7, pp. 2036–2040, Jul. 2014.

[8] D. S. Liebeskind, "Collateral circulation," *Stroke*, vol. 34, no. 9, pp. 2279–2284, 2003.

[9] S. Jung, R. Wiest, J. Gralla, R. McKinley, H. Mattle, and D. Liebeskind, "Relevance of the cerebral collateral circulation in ischaemic stroke: Time is brain, but collaterals set the pace," *Swiss Med. Weekly*, vol. 147, Dec. 2017, Art. no. w14538.

[10] R. Gonzalez, J. Hirsch, W. Koroshetz, M. Lev, and P. Schaefer, "Acute ischemic stroke: Imaging and intervention," *Amer. J. Neuroradiology*, vol. 28, no. 8, p. 1622, 2007.

[11] L. Østergaard, R. M. Weisskoff, D. A. Chesler, C. Gyldensted, and B. R. Rosen, "High resolution measurement of cerebral blood flow using intravascular tracer bolus passages. Part I: Mathematical approach and statistical analysis," *Magn. Reson. Med.*, vol. 36, no. 5, pp. 715–725, Nov. 1996.

[12] M. Bahr Hosseini and D. S. Liebeskind, "The role of neuroimaging in elucidating the pathophysiology of cerebral ischemia," *Neuropharmacology*, vol. 134, pp. 249–258, May 2018.

[13] K. Yamada, O. Wu, R. G. Gonzalez, D. Bakker, L. Østergaard, W. A. Copen, R. M. Weisskoff, B. R. Rosen, K. Yagi, T. Nishimura, and A. G. Sorensen, "Magnetic resonance perfusion-weighted imaging of acute cerebral infarction: Effect of the calculation methods and underlying vasculopathy," *Stroke*, vol. 33, no. 1, pp. 87–94, Jan. 2002.

[14] A. A. Konstas, G. V. Goldmakher, T.-Y. Lee, and M. H. Lev, "Theoretic basis and technical implementations of CT perfusion in acute ischemic stroke—Part 2: Technical implementations," *Amer. J. Neuroradiology*, vol. 30, no. 5, pp. 885–892, May 2009.

[15] F. Scalzo, Q. Hao, J. R. Alger, X. Hu, and D. S. Liebeskind, "Regional prediction of tissue fate in acute ischemic stroke," *Ann. Biomed. Eng.*, vol. 40, no. 10, pp. 2177–2187, Oct. 2012.

[16] S. E. Rose, J. B. Chalk, M. P. Griffin, A. L. Janke, F. Chen, G. J. McLachan, D. Peel, F. O. Zelaya, H. S. Markus, D. K. Jones, A. Simmons, M. O'Sullivan, J. M. Jarosz, W. Strugnell, D. M. Doddrell, and J. Semple, "MRI based diffusion and perfusion predictive model to estimate stroke evolution," *Magn. Reson. Imag.*, vol. 19, no. 8, pp. 1043–1053, Oct. 2001.

[17] R. McKinley, L. Häni, J. Gralla, M. El-Koussy, S. Bauer, M. Arnold, U. Fischer, S. Jung, K. Mattmann, M. Reyes, and R. Wiest, "Fully automated stroke tissue estimation using random forest classifiers (FASTER)," *J. Cerebral Blood Flow Metabolism*, vol. 37, no. 8, pp. 2728–2741, Aug. 2017.

[18] A. Nielsen, M. B. Hansen, A. Tietze, and K. Mouridsen, "Prediction of tissue outcome and assessment of treatment effect in acute ischemic stroke using deep learning," *Stroke*, vol. 49, no. 6, pp. 1394–1401, Jun. 2018.

[19] S. Winzeck, A. Hakim, R. McKinley, J. A. Pinto, V. Alves, C. Silva, M. Pisov, E. Krivov, M. Belyaev, M. Monteiro, and A. Oliveira, "Isles 2016 & 2017-benchmarking ischemic stroke lesion outcome prediction based on multispectral MRI," *Frontiers Neurol.*, vol. 9, p. 679, Sep. 2018.

[20] J. Amorim, A. Pinto, S. Pereira, and C. A. Silva, "Segmentation squeeze-and-excitation blocks in stroke lesion outcome prediction," in *Proc. IEEE 6th Portuguese Meeting Bioeng. (ENBENG)*, Feb. 2019, pp. 1–4.

[21] A. Pinto, S. Pereira, R. Meier, V. Alves, R. Wiest, C. A. Silva, and M. Reyes, "Enhancing clinical mri perfusion maps with data-driven maps of complementary nature for lesion outcome prediction," in *Medical Image Computing and Computer Assisted Intervention—MICCAI*. Cham, Switzerland: Springer, 2018, pp. 107–115.

[22] M. Giacalone, P. Rasti, N. Debs, C. Frindel, T.-H. Cho, E. Grenier, and D. Rousseau, "Local Spatio-temporal encoding of raw perfusion MRI for the prediction of final lesion in stroke," *Med. Image Anal.*, vol. 50, pp. 117–126, Dec. 2018.

[23] N. Debs, P. Rasti, L. Victor, T.-H. Cho, C. Frindel, and D. Rousseau, "Simulated perfusion MRI data to boost training of convolutional neural networks for lesion fate prediction in acute stroke," *Comput. Biol. Med.*, vol. 116, Jan. 2020, Art. no. 103579.

[24] M. Giacalone, C. Frindel, E. Grenier, and D. Rousseau, "Multicomponent and longitudinal imaging seen as a communication channel—An application to stroke," *Entropy*, vol. 19, no. 5, p. 187, Apr. 2017.

[25] M. Giacalone, C. Frindel, M. Robini, F. Cervenansky, E. Grenier, and D. Rousseau, "Robustness of Spatio-temporal regularization in perfusion MRI deconvolution: An application to acute ischemic stroke," *Magn. Reson. Med.*, vol. 78, no. 5, pp. 1981–1990, Nov. 2017.

[26] K. C. Ho, "Predicting ischemic stroke tissue fate using a deep convolutional neural network on source magnetic resonance perfusion images," *J. Med. Imag.*, vol. 6, no. 2, May 2019, Art. no. 026001.

[27] D. Robben, A. M. M. Boers, H. A. Marquering, L. L. C. M. Langezaal, Y. B. W. E. M. Roos, R. J. van Oostenbrugge, W. H. van Zwam, D. W. J. Dippel, C. B. L. M. Majoie, A. van der Lugt, R. Lemmens, and P. Suetens, "Prediction of final infarct volume from native CT perfusion and treatment parameters using deep learning," *Med. Image Anal.*, vol. 59, Jan. 2020, Art. no. 101589.

[28] K. Kamnitsas, C. Ledig, V. F. J. Newcombe, J. P. Simpson, A. D. Kane, D. K. Menon, D. Rueckert, and B. Glocker, "Efficient multi-scale 3D CNN with fully connected CRF for accurate brain lesion segmentation," *Med. Image Anal.*, vol. 36, pp. 61–78, Feb. 2017.

[29] R. McKinley, F. Hung, R. Wiest, D. S. Liebeskind, and F. Scalzo, "A machine learning approach to perfusion imaging with dynamic susceptibility contrast MR," *Frontiers Neurol.*, vol. 9, p. 717, Sep. 2018.
[30] A. Hess, R. Meier, J. Kaesmacher, S. Jung, F. Scalzo, D. Liebeskind, R. Wiest, and R. McKinley, "Synthetic perfusion maps: Imaging perfusion deficits in DSC-MRI with deep learning," 2018, *arXiv:1806.03848*. [Online]. Available: http://arxiv.org/abs/1806.03848
[31] F. Calamante, L. Willats, D. G. Gadian, and A. Connelly, "Bolus delay and dispersion in perfusion MRI: Implications for tissue predictor models in stroke," *Magn. Reson. Med.*, vol. 55, no. 5, pp. 1180–1185, 2006.
[32] O. Ronneberger, P. Fischer, and T. Brox, "U-Net: Convolutional networks for biomedical image segmentation," in *Proc. Int. Conf. Med. Image Comput. Computer-Assisted Intervent*. Cham, Switzerland: Springer, 2015, pp. 234–241.
[33] V. Nair and G. E. Hinton, "Rectified linear units improve restricted Boltzmann machines," in *Proc. ICML*, 2010, pp. 1–8.
[34] J. Tompson, R. Goroshin, A. Jain, Y. LeCun, and C. Bregler, "Efficient object localization using convolutional networks," in *Proc. IEEE Conf. Comput. Vis. Pattern Recognit. (CVPR)*, Jun. 2015, pp. 648–656.
[35] SMIR Online Platform. (2017). *Ischemic Stroke Lesion Segmentation 2017*. Accessed: Apr. 26, 2019. [Online]. Available: https://www.smir.ch/ISLES/Start2017
[36] N. J. Tustison, B. B. Avants, P. A. Cook, Y. Zheng, A. Egan, P. A. Yushkevich, and J. C. Gee, "N4ITK: Improved n3 bias correction," *IEEE Trans. Med. Imag.*, vol. 29, no. 6, pp. 1310–1320, Jun. 2010.
[37] F. Milletari, N. Navab, and S.-A. Ahmadi, "V-Net: Fully convolutional neural networks for volumetric medical image segmentation," in *Proc. 4th Int. Conf. 3D Vis. (3DV)*, Oct. 2016, pp. 565–571.
[38] K. Butcher and D. Emery, "Acute stroke imaging—Part I: Fundamentals," *Can. J. Neurolog. Sci./J. Canadien des Sci. Neurologiques*, vol. 37, no. 1, pp. 4–16, Jan. 2010.
[39] K. Butcher and D. Emery, "Acute stroke imaging—Part II: The ischemic penumbra," *Can. J. Neurological Sci./J. Canadien des Sci. Neurologiques*, vol. 37, no. 1, pp. 17–27, Jan. 2010.

ADRIANO PINTO (Member, IEEE) received the B.Sc. and master's degrees in biomedical engineering–medical electronics from the University of Minho, Portugal, in 2013 and 2015, respectively, and the joint Ph.D. degree in computer science from the Universities of Minho. His research interests include medical imaging, computer vision, machine learning, and representation learning.

JOANA AMORIM received the B.Sc. degree in 2017. She is currently pursuing the master's degree in biomedical engineering–medical electronics from the University of Minho, Portugal. Her master's thesis focuses on medical imaging and representation learning knowledge applied to predicting final infarct of an ischemic stroke.

ARSANY HAKIM is currently a Neuroradiologist with Bern University Hospital (INSEL). He cooperated closely in organizing the 2017 challenge edition of Ischemic Stroke Lesion Segmentation (ISLES). His clinical expertise encompasses cerebrovascular imaging, vessel wall imaging, and perfusion imaging. His research interest includes stroke imaging.

VICTOR ALVES is currently an Assistant Professor with the Department of Informatics, School of Engineering, University of Minho, and a Researcher with the Centro Algoritmi Research and Development Centre. His main research interest includes medical imaging informatics, mainly in modeling of the imaging modalities and their interpretation by synergistic human–machine methods for clinical benefits and applications not only in the computer-aided diagnosis/detection research context but also in the broader context of ambient intelligence.

MAURICIO REYES has been an Associate Professor with the Medical Imaging Analysis Faculty, University of Bern, since 2014. In 2008, he was the Head-Chief of the Medical Image Analysis Group, Institute for Surgical Technology and Biomechanics, Switzerland. He is currently the Head of the Healthcare Imaging A.I. Lab, Faculty of Medical, University of Bern. His research interests include machine learning for medical image analysis, neuroimaging, and interpretability of machine learning technologies for medical imaging.

CARLOS A. SILVA is currently an Assistant Professor with the Department of Electronics, School of Engineering, University of Minho. He is also a Researcher with the CMEMS-UMinho Research and Development Center. His research interests include intersection between machine learning and medical imagine processing, stroke tissue outcome prediction, brain tumor segmentation and grading, and retinal vessels segmentation.